Experimental and Theoretical Evidence for Subwavelength Imaging in Phononic Crystals

A. Sukhovich,[1] B. Merheb,[2] K. Muralidharan,[2] J. O. Vasseur,[3] Y. Pennec,[3] P. A. Deymier,[2] and J. H. Page[1]

[1]*Department of Physics and Astronomy, University of Manitoba, Winnipeg, Manitoba, R3T 2N2, Canada*
[2]*Department of Materials Science and Engineering, University of Arizona, Tucson, Arizona 85721, USA*
[3]*Institut d'Electronique, de Micro-électronique et de Nanotechnologie, UMR CNRS 8520, Cité Scientifique, 59652 Villeneuve d'Ascq Cedex, France*

(Received 7 July 2008; revised manuscript received 23 December 2008; published 17 April 2009)

We show experimentally and theoretically that super resolution can be achieved while imaging with a flat lens consisting of a phononic crystal exhibiting negative refraction. This phenomenon is related to the coupling between the incident evanescent waves and a bound slab mode of the phononic crystal lens, leading to amplification of evanescent waves by the slab mode. Super resolution is only observed when the source is located very near to the lens, and is very sensitive to the location of the source parallel to the lens surface as well as to site disorder in the phononic crystal lattice.

DOI: 10.1103/PhysRevLett.102.154301 PACS numbers: 43.35.+d, 63.20.−e

The possibility of achieving subwavelength resolution by focusing electromagnetic waves with a flat lens was first proposed eight years ago [1]. Such lenses exploit negative refraction of the incident waves in either left-handed metamaterials [1–3] or in photonic crystals [4–6]. In traditional imaging, the resolution of a lens is limited to half the wavelength λ by the loss of the evanescent component of the wave field emanating from the source. In left-handed metamaterials and photonic crystals, imaging with super resolution (better than the diffraction limit) may be possible with a flat lens if, for example, there is resonant coupling of the evanescent waves to bound surface or slab photon modes [4]. Recently, the concept of negative refraction and its application to focusing has been extended to acoustic waves [7–14]. Negative refraction of acoustic waves in phononic crystals (PCs) results from Bragg scattering and occurs in pass bands with negative group velocity (group velocity is opposite to the wave vector). Focusing of sound by either negative refraction [7–10,12–14] or by a canalization mechanism [15] has been recently shown with flat two-dimensional (2D) and three-dimensional PCs. However, with the exception of theoretical predictions for 2D PCs [10,15], the image resolution was worse than the diffraction limit.

As for left-handed metamaterials and photonic crystals, to achieve super resolution using PCs, it is necessary to enhance the evanescent field from the source. This has recently been shown theoretically for acoustic metamaterials where coupling to surface resonant modes was considered [16]. However, in spite of theoretical and experimental work demonstrating the presence of surface and slab modes in 2D PCs, their relevance to focusing has not been considered [17–23]. In this Letter, we demonstrate both experimentally and theoretically that super resolution can be achieved using a PC lens via the excitation of a bound slab mode. Our lens is constructed from a flat 2D triangular array of steel rods, in which all angle negative refraction (AANR) occurs. We show that the position of the source near the lens is critical to exciting the lens bound mode. We also report that disorder in the positions of the rods that make up the PC can be detrimental to the resolution of the lens. To our knowledge, this is the first experimental observation, in conjunction with theoretical predictions, of super resolution with PC lenses.

The 2D PC used in the imaging experiments was made of 1.02-mm-diameter stainless steel rods arranged in a triangular lattice with lattice parameter $a = 1.27$ mm. The surface of the crystal was covered by a very thin (0.01 mm) plastic film and the crystal was filled with methanol. When surrounded by water, this steel-methanol PC exhibits an effective refractive index of -1, due to matching circular equifrequency contours, at a frequency of 550 kHz [14]. For this crystal, AANR extends from this frequency down to the bottom of the second band at 500 kHz. A rectangular lens was constructed from 6 layers of rods, with 60 rods per layer, stacked in the ΓM direction of the Brillouin zone (BZ), i.e., with the base of the triangular cell parallel to the surface. The experiments were conducted in a water tank. The ultrasound source was a narrow subwavelength piezoelectric strip, 0.55 mm wide and 35 mm long, oriented with its long axis parallel to the steel rods; it was therefore an excellent approximation to a 2D point source. The spatiotemporal distribution of the acoustic field on the output side of the lens was detected with a miniature 0.40-mm-diameter hydrophone mounted on a motorized stage, which allowed the hydrophone to be scanned in a rectangular grid pattern. For subwavelength imaging, the source and detector widths must be smaller than λ at the frequency of interest; in our case, both are smaller than $\lambda/5$ in the AANR regime.

In Ref. [14], a resolution of 0.55λ was achieved at 550 kHz when the line source was located 1.6 mm from the crystal surface. To observe super resolution, we positioned the source significantly closer to the crystal surface at a distance of only 0.1 mm. We report in Fig. 1(a) the

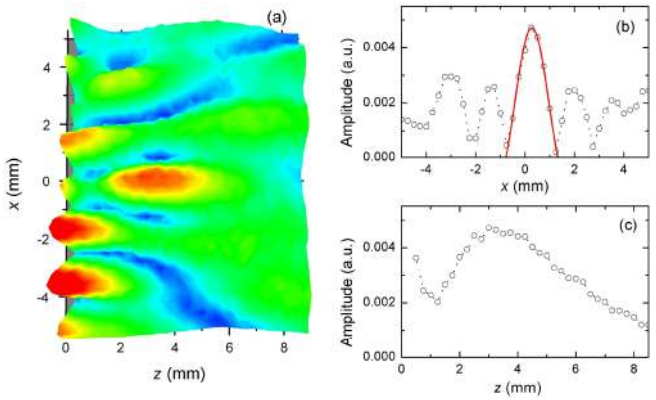

FIG. 1 (color online). (a) Three-dimensional map of experimental field amplitude on the imaging side of the water-methanol-steel flat lens at a frequency of 530 kHz. (b) Field amplitude through the focus along the direction parallel to the lens surface. The data fit to a sinc function (solid line) gives a half width of the primary peak, $\Delta/2$, of 0.37λ. (c) Field amplitude through the focus along the direction perpendicular to the lens surface. The surface is located at $z = 0$.

scanned map of the field amplitude at 530 kHz, obtained from the Fourier transform at this frequency of the hydrophone signal at each spatial position. Figure 1(a) shows a distinct focal spot with additional near-periodic peaks that are largest next to the crystal surface. These additional peaks decay rapidly with distance from the surface, revealing the presence of a mode that is bound to the PC slab and is only excited by the source when it is placed close to the surface {compare Fig. 1(a) with Fig. 10(a) of Ref. [14]}. These peaks also show up as sidelobes flanking the central image peak in the cross section of the field through the focal spot parallel to the lens [Fig. 1(b)]. The focal spot itself is located approximately 3.0 mm from the crystal surface [Fig. 1(c)]. The full width of the focal spot was measured by fitting the central peak in Fig. 1(b) by the usual sinc function, $\mathrm{sinc}(2\pi x/\Delta)$, giving a resolution $\Delta/2$, as defined by the Rayleigh criterion, of 1.05 mm or 0.37λ. This resolution is clearly less than the ultimate resolution limit $\lambda/2$ of a conventional imaging system. The focus pattern changes with the position of the source along the surface of the crystal. The image in Fig. 1 corresponds to the best case among several super resolution images measured for different lateral source positions.

We study theoretically the imaging properties of the methanol-steel PC lens with the Finite Difference Time Domain (FDTD) method. The FDTD method can calculate the propagation of acoustic waves in PCs [24,25], as well as their band structure [26]. For band structure calculations, periodic boundary conditions are applied in all directions. We use an interval for the discretization of space of 2×10^{-5} m. The time step is 6×10^{-10} s. These values satisfy the Courant condition and lead to a stable algorithm. The calculations were conducted with the following data for the constitutive materials: steel (mass density, $\rho = 7890$ kg/m^3, longitudinal and transverse sound speeds, $v_l = 5800$ m/s and $v_t = 3100$ m/s); methanol ($\rho = 790$ kg/m^3 and $v_l = 1138$ m/s); water ($\rho = 1000$ kg/m^3 and $v_l = 1490$ m/s). The calculated band structure of the periodic PC in the ΓM direction of the irreducible BZ are compared with our experimental results in Fig. 2. The band structure exhibits a pass band between approximately 500 and 800 kHz with a negative group velocity. The existence of a stop band along the ΓM direction between 400 and 500 kHz is confirmed by measurements and FDTD calculations of the transmission coefficient for a 6-layer crystal (Fig. 2, right panel). Excellent agreement between theory and experiment is found for both the band structure and transmission coefficient.

The FDTD lens was modeled as a PC slab with the same lateral extent ($60a$) and the same number of layers (6) as the experimental crystal. We use a line source (0.55 mm wide) running parallel to the principal axis of the steel cylinders. The mesh points belonging to the source emit a sinusoidal displacement of frequency ν, with components parallel and perpendicular to the surface of the lens. We impose Mur's absorbing boundary conditions [27] along the four edges of the simulated system. We conducted a series of simulations with various ν near the bottom of the second band and various distances between the lens and the source. Optimal imaging conditions were obtained for a source frequency of 530 kHz and a source-to-lens distance of 0.1 mm (Fig. 3). This image exhibits traits similar to those observed experimentally (Fig. 1). The field distribution along a line parallel to the lens surface shows many closely spaced, nearly periodic peaks [Figs. 1(b) and 3(b)].

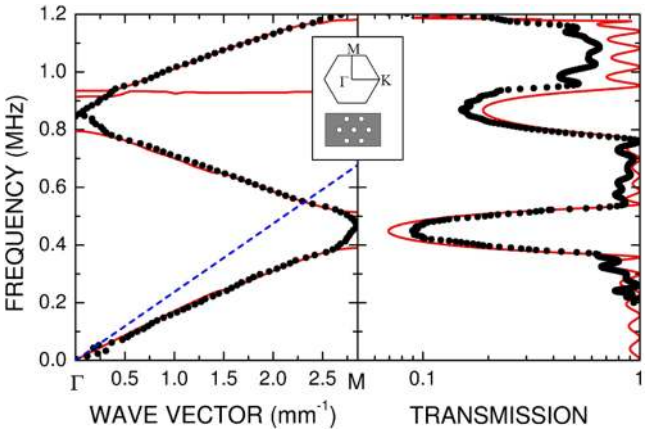

FIG. 2 (color online). Band structure of the methanol-steel PC in the ΓM direction of the first BZ (left panel) and transmission coefficient for a 6-layer crystal along the same direction (right panel): symbols, experimental data; solid lines, FDTD calculation; dashed line, homogeneous water. The inset illustrates the phononic crystal structure and the associated first Brillouin zone.

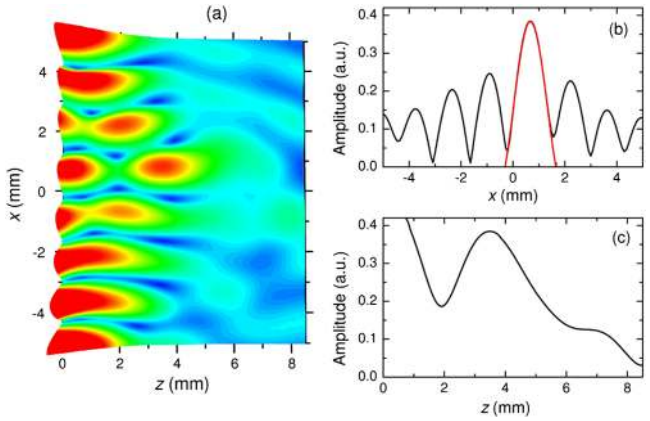

FIG. 3 (color online). (a) Three-dimensional map of the normalized average absolute value of pressure calculated via the FDTD method. The source frequency is 530 kHz. (b) Normalized average absolute value of the pressure along a line parallel to the lens through the center of the focal point. The half-width $\Delta/2$ of the primary peak is 0.35λ. The offset in lateral position of the focus is due to the FDTD staggered grid that ensures numerical stability. (c) Same as (b) but along a direction perpendicular to the lens. The surface of the lens is located at $z = 0$.

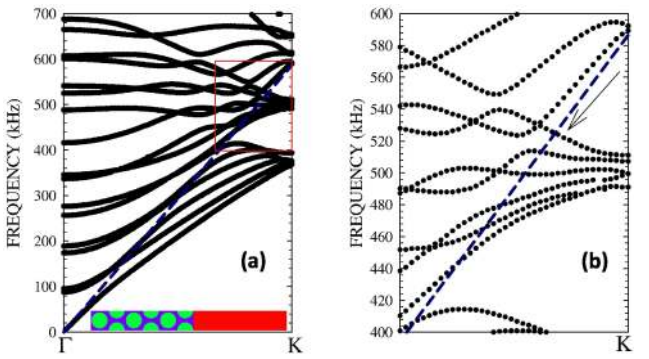

FIG. 4 (color online). (a) Calculated band structure of methanol-steel PC slab immersed in water (inset: phononic crystal, left block; water, right block) for wave vectors parallel to the slab surface (transverse wave vector along ΓK direction). The long dashed line corresponds to sound propagation in water. (b) Magnification of the region enclosed by the box in (a). The arrow points to a bound slab phonon mode near 510 kHz.

The half-width of the predicted central peak is 0.35λ, in very good agreement with the experimentally observed resolution. The field in Fig. 3(c) shows a clear maximum at approximately 3.5 mm from the exit surface of the lens—also in good accord with experimental observations. Calculations performed for different numbers of rods or layers (15 and 51) gave similar results, so long as the absorbing boundary conditions were applied. Calculations were also performed to investigate the dependence of image quality on the number of layers; these calculations revealed that the optimum number of layers is 6, since in this case the image is close enough to the lens surface to take advantage of the evanescent contribution to image formation while not being so close to the lens surface that the image is swamped by the bound crystal mode.

In the experiment and calculations, super resolution is only achieved for a source in very close proximity to the lens surface, which is consistent with the possibility of exciting a bound slab vibrational mode. To shed light on the origin of the super resolution, we have calculated the band structure over transverse wave vectors of the finite PC slab immersed in water—see Fig. 4. The inset represents the supercell used for this calculation. The water layer is sufficiently thick to avoid overlap of bound slab modes arising from the periodicity imposed by the FDTD method for calculating band structures. In Fig. 4, the modes that lie below the water line are bound slab modes as they cannot propagate in water. They propagate along the principal direction of the PC slab (i.e., the ΓK direction). Amplification of evanescent waves arises when the operation frequency (530 kHz) is close to the frequency of a bound mode. Of particular interest is the bound slab mode marked with an arrow in Fig. 4(b). This mode extends from 525 kHz at the water line to 510 kHz at the edge of the BZ and is very close to our operation frequency. Coupling between the waves emitted by the source and this mode gives rise to enhancement of the evanescent field and therefore a reconstruction of the image beyond the diffraction limit. Optimum focusing is observed at 530 kHz since this represents the best compromise between perfect matching of the equifrequency contours and sufficient proximity to the bound mode that it can be excited. Luo *et al.* have studied theoretically a similar coupling in the case of a photonic crystal lens [4]. These authors estimated the ultimate resolution limit, $\Delta/2$, of a photonic crystal superlens, due to the amplification of evanescent waves by a bound mode, to lie in the interval $[0.5a_s\lambda/(\lambda - a_s), a_s]$, where a_s is the period of the lattice parallel to the surface of the lens. Applying this estimate to our PC with $a_s = 1.27$ mm, and a wavelength in water at 530 kHz of 2.81 mm, the minimum feature size that would be resolvable ranges in the interval $[0.41\lambda, 0.45\lambda]$. Thus, their lower limit is larger than our experimental and numerical results, implying that modes with transverse wave vectors larger than those considered in Luo *et al.*'s simple estimate are excited in our PC.

Figure 5(a) shows the calculated average pressure field both inside and outside the lens at 530 kHz. The large pressure amplitude in the vicinity of the rods extends over the entire slab, and is characteristic of the excitation of a mode that is bound to the slab. Super resolution is lost when the source is displaced parallel to the surface by $a_s/2$ [Fig. 5(b)], where it is unable to couple effectively to the bound mode of the lens. In this case, the pressure field is clearly localized within the central part of the lens. The image in Fig. 5(b), which has a resolution of approximately 0.5λ, is reconstructed from propagating waves that are negatively refracted in the PC slab.

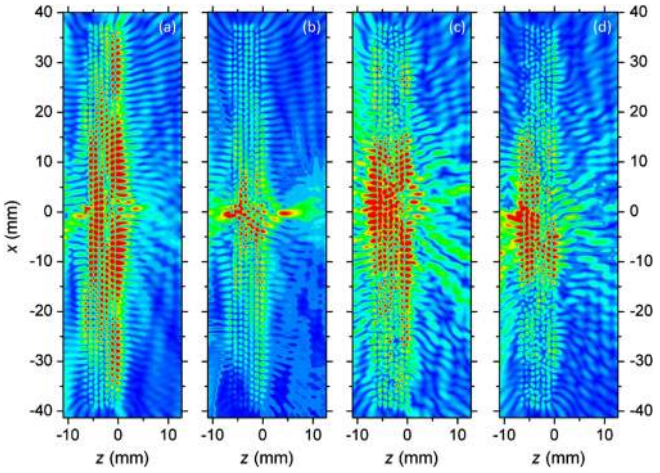

FIG. 5 (color online). Contour maps of the normalized average absolute value of pressure calculated via FDTD (a) at a frequency of 530 kHz for the PC lens imaging the 0.55-mm-wide line source located at 0.1 mm from the left lens surface and centered with respect to a surface cylinder at $x = 0$, (b) same as (a) but with the source shifted down by $a_s/2$ in the direction parallel to the surface of the lens, and (c), (d) for two lenses with positional disorder of the steel rods showing imperfect focusing (c) and loss of focusing (d). The positional disorder in the numerical model has a standard deviation of 5%, which corresponds to an upper limit for the experimental crystal, as the disorder was measured only on the surface. Because of the fabrication method, the disorder at the surface is greater than in the interior.

The experimental measurements were found to be very sensitive to disorder in the position of the steel rods. We confirm in Figs. 5(c) and 5(d) that disorder in the PC is detrimental to the quality of the image and for some random realizations, can even eliminate the focusing property of the lens.

In summary, this Letter provides strong experimental and theoretical evidence for super resolution using flat lenses made from PCs. The super resolution is achieved by excitation of a bound mode of the lens, which permits the amplification of evanescent components of the source field. The observed resolution for this PC is 30% lower than the diffraction limit, and, as a fraction of the wavelength, is somewhat better than the ultimate resolution predicted for photonic crystals by Luo *et al.* [4]. Our results may be viewed as a validation of the basic mechanisms that have been proposed for super resolution to be achieved in any flat crystal lens, whether phononic or photonic.

We thank NSERC of Canada for its support, and Anatoliy Strybulevych for measuring the ultrasonic velocity of the methanol used in our PC.

[1] J. B. Pendry, Phys. Rev. Lett. **85**, 3966 (2000).
[2] N. Garcia and M. Nieto-Vesperinas, Phys. Rev. Lett. **88**, 207403 (2002).
[3] G. Gomez-Santos, Phys. Rev. Lett. **90**, 077401 (2003).
[4] C. Luo, S. G. Johnson, J. D. Joannopoulos, and J. B. Pendry, Phys. Rev. B **68**, 045115 (2003).
[5] E. Cubukcu, K. Aydin, E. Ozbay, S. Foteinopolou, and C. M. Soukoulis, Phys. Rev. Lett. **91**, 207401 (2003).
[6] Z. Lu, J. A. Murakowski, C. A. Schuetz, S. Shi, G. J. Schneider, and D. W. Prather, Phys. Rev. Lett. **95**, 153901 (2005).
[7] S. Yang, J. H. Page, Z. Liu, M. L. Cowan, C. T. Chan, and P. Sheng, Phys. Rev. Lett. **93**, 024301 (2004).
[8] J. H. Page, A. Sukhovich, S. Yang, M. L. Cowan, F. Van der Biest, A. Tourin, M. Fink, Z. Liu, C. T. Chan, and P. Sheng, Phys. Status Solidi (b) **241**, 3454 (2004).
[9] K. Imamura and S. Tamura, Phys. Rev. B **70**, 174308 (2004).
[10] X. Zhang and Z. Liu, Appl. Phys. Lett. **85**, 341 (2004).
[11] J. Li and C. T. Chan, Phys. Rev. E **70**, 055602 (2004).
[12] J. Li, K. H. Fung, Z. Y. Liu, P. Sheng, and C. T. Chan, in *Physics of Negative Refraction and Negative Index Materials*, Springer Series in Materials Science, Vol. 98, Chap. 8 (Springer, Berlin, Heidelberg, 2007).
[13] M. Ke, Z. Liu, Z. Cheng, J. Li, P. Peng, and J. Shi, Solid State Commun. **142**, 177 (2007).
[14] A. Sukhovich, L. Jing, and J. Page, Phys. Rev. B **77**, 014301 (2008).
[15] Z. He, F. Cai, Y. Ding, and Z. Liu, Appl. Phys. Lett. **93**, 233503 (2008).
[16] M. Ambati, N. Fang, C. Sun, and X. Zhang, Phys. Rev. B **75**, 195447 (2007).
[17] Y. Tanaka and S. Tamura, Phys. Rev. B **58**, 7958 (1998).
[18] T. T. Wu, Z. G. Huang, and S. Lin, Phys. Rev. B **69**, 094301 (2004).
[19] C. Charles, B. Bonello, and F. Ganot, Ultrasonics **44**, e1209 (2006).
[20] J. C. Hsu and T. T. Wu, Phys. Rev. B **74**, 144303 (2006).
[21] J. O. Vasseur, P. A. Deymier, B. Djafari-Rouhani, Y. Pennec, and A.-C. Hladky-Hennion, Phys. Rev. B **77**, 085415 (2008).
[22] T. T. Wu, L. C. Wu, and Z. G. Huang, J. Appl. Phys. **97**, 094916 (2005).
[23] B. Manzanares-Martinez and F. Ramos-Mendieta, Phys. Rev. B **68**, 134303 (2003).
[24] D. Garcia-Pablos, M. Sigalas, F. R. Montero de Espinosa, M. Torres, M. Kafesaki, and N. Garcia, Phys. Rev. Lett. **84**, 4349 (2000).
[25] J. O. Vasseur, P. A. Deymier, B. Chenni, B. Djafari-Rouhani, L. Dobrzynski, and D. Prevost, Phys. Rev. Lett. **86**, 3012 (2001).
[26] Y. Tanaka, Y. Tomoyasu, and S. Tamura, Phys. Rev. B **62**, 7387 (2000).
[27] G. Mur, IEEE Trans. Electromagn. Comput. **emc-23**, 377 (1981).